nature mental health

Article

https://doi.org/10.1038/s44220-025-00522-3

The BMIgap tool to quantify transdiagnostic brain signatures of current and future weight

Received: 14 October 2024

Accepted: 18 September 2025

Published online: 20 October 2025

Check for updates

Adyasha Khuntia[1,2,3,28], David Popovic[1,3,28], Elif Sarisik[1,2,3], Madalina O. Buciuman[1,2,3], Mads L. Pedersen[4], Lars T. Westlye[4,5,6], Ole A. Andreassen[5,6], Andreas Meyer-Lindenberg[7,8], Joseph Kambeitz[9], Raimo K. R. Salokangas[10], Jarmo Hietala[10], Alessandro Bertolino[11], Stefan Borgwardt[12,13], Paolo Brambilla[14,15], Rachel Upthegrove[16,17,18,19], Stephen J. Wood[20,21,22], Rebekka Lencer[12,23], Eva Meisenzahl[24], Peter Falkai[1,3,25], Emanuel Schwarz[7,8,26], Ariane Wiegand[1,3,28] & Nikolaos Koutsouleris[1,3,25,27,28]

Understanding the neurobiological underpinnings of weight gain could reduce excess mortality and improve long-term trajectories of psychiatric disorders. Using brain scans from healthy individuals (n = 1,504), we trained a model to predict body mass index (BMI) and applied it to individuals with schizophrenia (n = 146), clinical high-risk states for psychosis (n = 213) and recent-onset depression (ROD, n = 200). We computed BMIgap ($BMI_{predicted} - BMI_{measured}$), interrogated its brain-level overlaps with schizophrenia and explored whether BMIgap predicted weight gain at the 1-year and 2-year follow-ups. Schizophrenia (BMIgap = 1.05 kg m^{-2}) and clinical high-risk individuals (BMIgap = 0.51 kg m^{-2}) showed increased BMIgap and individuals with ROD (BMIgap = −0.82 kg m^{-2}) showed decreased BMIgap. Shared brain patterns of BMI and schizophrenia were linked to illness duration, disease onset and hospitalization frequency. Higher BMIgap predicted future weight gain, particularly in younger individuals with ROD, and at 2-year follow-up. Here we show that BMIgap can serve as a potential brain-derived measure to stratify at-risk individuals and deliver tailored interventions for better metabolic risk control.

Globally, 26% of adults are overweight (body mass index (BMI) = 25–30 kg m^{-2}) with an additional 13% classified as obese (BMI ≥ 30 kg m^{-2})[1], highlighting the pandemic nature of obesity[2,3]. Given its strong associations with metabolic diseases, including cardiovascular disease and type 2 diabetes, obesity stands as a major risk factor for somatic disorders[4]. Importantly, obesity frequently parallels psychiatric disorders such as schizophrenia, major depressive disorder, bipolar disorder and personality and anxiety disorders[5,6]. Psychiatric patients have a twofold to threefold higher incidence of obesity and metabolic diseases compared to the general population, substantially contributing to their excess mortality[7,8]. Secondary factors such as smoking, alcohol use, sedentary lifestyle and commonly prescribed medications also markedly affect body weight and metabolic syndromes in psychiatric patients[9,10]. In particular, atypical antipsychotics and antidepressants have been implicated in weight gain[11,12]. Furthermore, individuals exhibiting negative symptoms, which are characterized by affective flattening, anhedonia and avolition, are at an increased risk for weight gain[13]. In turn, weight gain and obesity can have a negative impact on the quality of life and self-esteem of affected individuals, thereby further exacerbating already preexisting mental health issues and ultimately leading to a vicious circle between psychiatric symptoms, secondary disease effects and weight gain[14,15].

A full list of affiliations appears at the end of the paper. e-mail: nikolaos.koutsouleris@med.uni-muenchen.de

In healthy populations, neuroimaging studies have identified associations between higher BMI and reduced gray matter volume (GMV) in the prefrontal, temporal, parietal and occipital cortices, the cerebellum, insula, thalamus and amygdala[16–18]. These group-level associations might be related to lowered inhibitory control of food-related stimuli resulting from a dysbalance of brain activity in neural systems responsible for cognitive control and reward[17–19]. These findings suggest a plausible relationship between cognitive control deficits and overeating[19], potentially resulting in higher caloric intake and obesity[17]. Furthermore, in patients with schizophrenia, higher BMI was associated with reduced GMV in the prefrontal cortex, specifically the orbitofrontal cortex, and the hippocampus[20]. In patients with major depressive disorder, higher BMI was correlated with reduced GMV in the medial prefrontal regions, particularly in areas involved in impulse control and emotion regulation[21]. These brain regions are crucial for impulse control and reward processing, suggesting a shared neural basis underlying both psychiatric symptomatology and metabolic dysregulation[22–24]. Furthermore, individuals with schizophrenia exhibit the highest risk for developing metabolic comorbidities among patients with psychiatric disorders. These comorbidities reduce life expectancy up to 25 years in these patients compared to the general population, effects that cannot be explained by medication effects alone[25,26].

Despite these advances, most existing studies have relied on group-level comparisons, which do not detect individualized deviations from the normative brain–BMI relationship. However, an individualized approach is essential to move beyond population averages and to identify person-specific complex neural markers of metabolic risk. Addressing this gap is especially important in schizophrenia, where metabolic vulnerability may arise from neurobiological alterations that are common to both metabolic and psychiatric disorders. Investigating whether the GMV patterns that predict BMI also contribute to schizophrenia-specific neural changes will provide a framework to examine shared neurobiological mechanisms and quantify brain-based metabolic vulnerability[27,28]. Developing these tools could help detect early alterations in brain–BMI interactions and facilitate targeted interventions, such as exercise, psychotherapy, medications or brain stimulation, to prevent weight gain, improve treatment adherence and reduce excess mortality[29,30].

To address the knowledge gap in how brain structure relates to BMI in psychiatric disorders, we implemented a normative modeling framework to predict BMI at the individual level using whole-brain GMV trained on a large discovery sample of healthy control (HC) individuals ($HC_{discovery}$). We validated this BMI predictor model in two independent HC samples ($HC_{validation}$ and $HC_{Cam\text{-}CAN}$) to measure its generalizability to new, unseen individuals. We then applied the model to clinical groups, including individuals with schizophrenia, recent-onset depression (ROD) and clinical high-risk (CHR) states for psychosis, to examine how brain-based BMI predictions deviate from the reference. The resulting metric, BMIgap ($BMI_{predicted} - BMI_{measured}$), captures individualized brain-based deviations that may reflect metabolic vulnerability toward higher or lower BMI. By comparing BMIgap across clinical groups, we explored whether psychiatric disorders are characterized by systematic deviations in brain–BMI associations, offering new insights into the neurobiological differences underlying metabolic alterations in different psychiatric disorders. Next, to investigate whether BMIgap captures structural brain deviations relevant to schizophrenia and its clinical expression, we examined the phenotypic association between BMIgap, schizophrenia expression (that is, neuroanatomical similarity to schizophrenia) and clinical features using sparse partial least squares (SPLS). Furthermore, to assess the clinical relevance of BMIgap in metabolic outcomes, we correlated it with future weight changes at the 1-year and 2-year follow-ups at the group level and incorporated it alongside additional clinical factors to predict individual weight gain trajectories. We hypothesized that (1) accurate models for individualized BMI prediction can be derived from structural brain imaging using supervised machine learning, (2) interactions between BMI-predictive and disease-specific brain signatures result in systematic brain deviations that are captured by BMIgap, (3) BMIgap is associated with key measures of disease severity, including age at onset, illness duration or hospitalization frequency, and (4) BMIgap can serve as a personalized brain-based tool to assess future weight gain and identify at-risk individuals in the early disease stages.

Results

Individualized BMI prediction

Sociodemographic characteristics of the discovery, validation, Cam-CAN and patient groups are summarized in Table 1. The model predicted BMI in $HC_{discovery}$ individuals with a mean absolute error (MAE) of 2.75 kg m^{-2} ($R^2 = 0.28$, $P < 0.001$) and generalized to the $HC_{validation}$ with an MAE of 2.29 kg m^{-2} ($R^2 = 0.26$, $P < 0.001$) as well as $HC_{Cam\text{-}CAN}$ with an MAE of 2.96 kg m^{-2} ($R^2 = 0.32$, $P < 0.001$) (Fig. 1a). Applied to the clinical subpopulations, the BMI predictor yielded an MAE of 2.85 kg m^{-2} for schizophrenia ($R^2 = 0.25$, $P < 0.001$), an MAE of 3.07 kg m^{-2} for CHR ($R^2 = 0.16$, $P < 0.001$) and an MAE of 2.73 kg m^{-2} for ROD ($R^2 = 0.10$, $P < 0.001$) individuals (Table 2 and Fig. 1b).

Lower GMV in the cerebellar, prefrontal (including the ventromedial prefrontal cortex), occipital and insular cortices, as well as the postcentral gyrus, hippocampus, thalamus, putamen and pallidum (core components of the ventral striatum) and cingulate cortex (involved in reward anticipation, valuation and inhibitory control), was predictive of higher BMI. Lower GMV in the left hemisphere involving the cingulate, cerebellar, inferior occipital and temporal cortices, as well as in the right hemisphere covering parts of the precuneus, putamen and Rolandic operculum were predictive of lower BMI (Fig. 1c, Supplementary Fig. 5 and Supplementary Table 3).

BMIgap estimation across clinical groups

The application of the BMI predictor yielded a mean (±s.d.) BMIgap of 0.23 (±1.68) kg m^{-2} for $HC_{validation}$, 0.24 (±3.26) kg m^{-2} for $HC_{Cam\text{-}CAN}$, 1.05 (±1.53) kg m^{-2} for schizophrenia, −0.82 (±1.64) kg m^{-2} for ROD and 0.51 (±1.68) kg m^{-2} for CHR individuals. BMIgap differed between $HC_{discovery}$ and $HC_{validation}$ individuals and clinical groups (Fig. 1d; $F_{(discovery\ versus\ patients)} = 33.90$, $P < 0.001$; $F_{(validation\ patients)} = 32.36$, $P < 0.001$). Notably, post hoc pairwise comparisons revealed significant differences in BMIgap between the $HC_{discovery}$ and $HC_{validation}$ groups ($t = 2.62$, $P = 0.009$) probably because of variations in BMI distributions, as indicated by a significant difference in variances ($F = 3.8018$, $P < 0.001$; Supplementary Fig. 1a,c). However, BMIgap did not differ between $HC_{discovery}$ and $HC_{Cam\text{-}CAN}$ ($t = 1.78$, $P = 0.08$) as well as $HC_{validation}$ and $HC_{Cam\text{-}CAN}$ ($t = -0.11$, $P = 0.92$) (Fig. 1d). BMIgap differed significantly between $HC_{discovery}$ and all clinical groups, with the highest BMIgap for schizophrenia ($t = 6.68$, $P < 0.001$), followed by CHR ($t = 3.72$, $P < 0.001$) and the lowest for ROD ($t = -5.88$, $P < 0.001$).

We did not find significant differences in BMIgap between medication-naive ($n = 80$, 37.56%), antipsychotic-naive ($n = 153$, 71.83%), antidepressant-naive ($n = 108$, 50.70%) and concurrently antidepressant-antipsychotic-treated ($n = 133$, 62.44%) within CHR individuals ($F = 0.6$, $P = 0.6244$). Similarly, no significant differences were observed between the BMIgap of medication-naive ($n = 59$, 29.50%), antipsychotic-naive ($n = 173$, 86.50%), antidepressant-naive ($n = 63$, 31.50%) and concurrently antidepressant-antipsychotic-treated ($n = 141$, 70.50%) individuals with ROD ($F = 0.002$, $P = 0.9964$). Furthermore, BMIgap did not significantly differ between individuals receiving weight gain medications ($n_{CHR} = 81$ (47.65%), $n_{ROD} = 92$ (52.27%), $n_{CHR+ROD} = 173$ (50%)) and those on weight-neutral or no medications ($n_{CHR} = 28$ (16.47%), $n_{ROD} = 20$ (11.36%), $n_{CHR+ROD} = 48$ (13.87%)) within the CHR ($t = 0.6068$, $P = 0.5448$) and ROD ($t = 1.2187$, $P = 0.2246$) groups, nor in the combined CHR and ROD sample ($t = 0.8445$, $P = 0.3990$) (Supplementary Fig. 10). Moreover, we did not find a significant correlation between BMIgap and chlorpromazine equivalents ($r = -0.01$, $P = 0.86$) in the schizophrenia sample.

https://doi.org/10.1038/s44220-025-00522-3

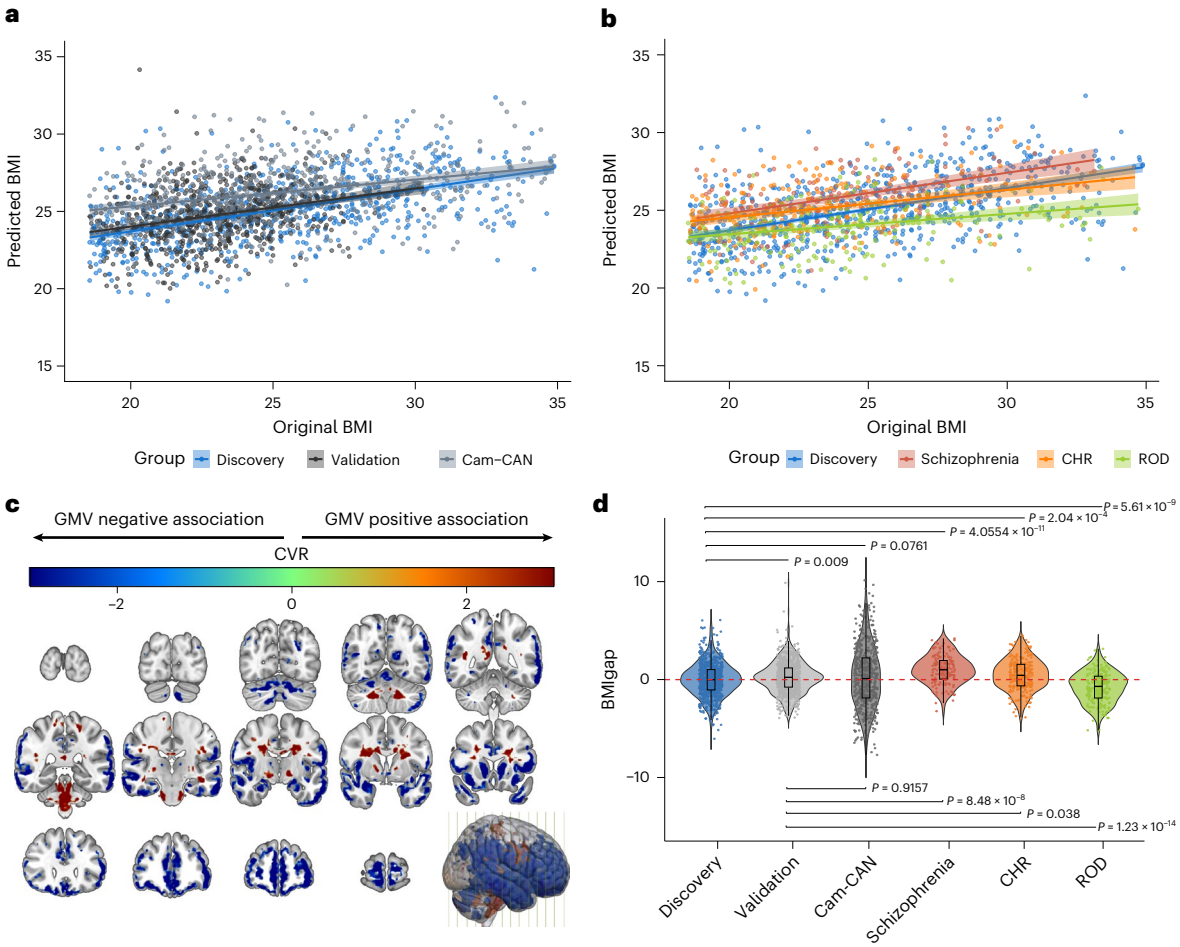

Fig. 1 | Visualization and performance of the BMI predictor. a, Original BMI score versus predicted BMI score with a linear curve fit; the regression line is shown with the ±95% confidence interval (CI) of the mean BMI prediction for the discovery group (blue), validation group (black) and Cam-CAN group (gray). **b**, Original BMI score versus predicted BMI score with a linear curve fit; the regression line with ±95% CI of the mean BMI prediction for the discovery group (blue), patients with schizophrenia (dark orange), CHR individuals (light orange) and individuals with ROD (yellow). **c**, Reliability of the predictive voxels visualized using a grand mean cross-validation ratio (CVR) map thresholded based on the false discovery rate (FDR)-corrected, sign-based consistency map at $\alpha = 0.05$. Cool colors indicate voxels with a negative association of GMV and estimated BMI; warm colors represent a positive correlation. **d**, Box plots of BMIgap for the different study groups, including discovery ($n = 770$), validation ($n = 734$), Cam-CAN ($n = 536$), schizophrenia ($n = 146$), CHR ($n = 213$) and ROD ($n = 200$). The box plots show the median (center line), interquartile range (IQR) (box edges) and whiskers extending to 1.5 times the IQR. BMIgap differences among groups were tested using a two-sided analysis of variance ($F = 15.97$, d.f. = 5, 2,593, $P = 1.59 \times 10^{-15}$).

Schizophrenia-specific brain signatures

The schizophrenia classifier yielded a balanced accuracy (BAC) of 72.4% (sensitivity = 72.2%, specificity = 72.6%; $P < 0.001$) in separating HCs from individuals with schizophrenia. Voxels predictive of schizophrenia were found predominantly in the inferior, middle and superior frontal gyrus, as well as in hippocampal, thalamic, insular, Rolandic operculum, postcentral, cerebellar and basal ganglia structures. In the right hemisphere, the lingual, fusiform gyrus and mid-temporal lobe were predictive of schizophrenia class membership (Supplementary Fig. 6). The brain patterns of the BMI predictor and the schizophrenia classifier overlapped in the inferior, middle and superior frontal gyrus, caudate, putamen, Rolandic operculum, right precuneus and the middle temporal lobe regions (Supplementary Fig. 7).

Clinical associations of shared schizophrenia and BMI signatures

The SPLS analysis yielded five reliable latent variables (LVs), representing distinct levels of association between the neuroanatomic overlap regions of the BMI and schizophrenia models, and the clinical disease features (Fig. 2 and Supplementary Fig. 8). While LV2, LV3 and LV5 captured disease-specific patterns, LV1 and LV4 extracted covariate patterns of age and sex (Supplementary Results).

In LV2 ($r = 0.84$, $P < 0.001$), higher BMIgap, schizophrenia expression scores, age at onset, number of hospitalizations and illness duration were related to decreased GMV in the default mode network (DMN) specifically in the A, B and C subcomponents, visual, somatomotor A, attention, salience, limbic, and control networks, and increased GMV in the DMN (auditory) and somatomotor B networks (Fig. 2a).

In LV3 ($r = 0.85$, $P < 0.001$), higher BMIgap and higher schizophrenia expression scores were related to decreased GMV in the DMN-B and increased GMV in the DMN D (auditory) (Fig. 2b).

In LV5 ($r = 0.58$, $P < 0.001$), lower PANSS total score, illness duration and age at onset, and higher schizophrenia expression score were related to decreased GMV in DMN-C and control-C networks, and increased GMV in the DMN-A/B, somatomotor B, dorsal attention-B and salience networks (Fig. 2c).

BMIgap and future weight change

In HC individuals, BMIgap showed a positive correlation with a 2-year weight gain (ΔW_2, $n = 216$; $r = 0.14$, $P_{FDR} = 0.0347$); specifically, in the subgroup of adults between 25 and 40 years (N = 46; $r = 0.46$, $P_{FDR} = 0.034$).

https://doi.org/10.1038/s44220-025-00522-3

Table 1 | Sociodemographic differences in the discovery, validation, Cam-CAN and patient groups

	HC			*F*/Chi-squared	*P*	Clinical group			*F*/Chi-squared	*P*
	Discovery	Validation	Cam-CAN			Schizophrenia	CHR	ROD		
Sample (*n*)	770	734	536	46.69[a]	**7.253×10^{-11}**	146	213	200	776.60[a]	**2.2×10^{-16}**
BMI, mean (s.d.)	25.10 (4.03)	23.03 (2.07)	25.43 (3.64)	104.8[b]	**4.7637×10^{-44}**	24.02 (3.40)	23.46 (3.42)	24.01 (3.57)	13.48[b]	**1.1456×10^{-8}**
Age, mean (s.d.)	41.26 (15.51)	32.24 (12.75)	54.26 (18.56)	313.44[b]	**2.0873×10^{-119}**	30.83 (9.97)	23.92 (5.24)	26.02 (6.37)	164.42[b]	**3.2518×10^{-86}**
Sex, female, *n* (%)	435 (56.49)	373 (50.82)	261 (48.69)	43.65[a]	**3.32×10^{-10}**	34.00 (23.29)	103 (48.36)	96 (48.00)	590.72[a]	**2.2×10^{-16}**
Symptoms, mean (s.d.)										
PANSS (total)	NA	NA	NA	NA	NA	52.26 (29.45)	52.07 (18.22)	48.44 (14.26)	2.08[b]	0.13
PANSS (positive)	NA	NA	NA	NA	NA	11.92 (8.13)	11.31 (4.16)	8.20 (2.21)	29.09[b]	**9.6792×10^{-13}**
PANSS (negative)	NA	NA	NA	NA	NA	14.98 (9.73)	13.09 (6.86)	12.50 (5.66)	5[b]	**0.007**
PANSS (general)	NA	NA	NA	NA	NA	25.36 (16.13)	27.66 (10.05)	27.74 (8.84)	2.19[b]	0.113
SANS (total)	NA	NA	NA	NA	NA	44.44 (26.52)	27.08 (24.88)	23.91 (20.95)	30.69[b]	**2.4128×10^{-13}**
BDI	3.55 (5.05)	3.27 (5.20)	NA	0.50[c]	0.616	NA	24.09 (11.75)	24.56 (12.48)	182.47[b]	**3.5659×10^{-60}**
Functioning, mean (s.d.)										
GAF:S past month	86.30 (6.43)	87.32 (6.16)	NA	1.54[c]	0.124	NA	51.31 (11.29)	53.92 (13.17)	503.97[b]	**3.0021×10^{-125}**
GAF:D past month	85.49 (6.32)	86.51 (5.89)	NA	1.59[c]	0.113	NA	51.94 (12.)	54.14 (3.60)	385.24[b]	**1.8717×10^{-105}**
GF:S current	8.50 (0.89)	8.54 (0.71)	NA	0.51[c]	0.612	NA	6.25 (1.75)	6.39 (1.23)	157.82[b]	**6.7860×10^{-55}**
GF:R current	8.49 (0.77)	8.59 (0.67)	NA	1.40[c]	0.164	NA	5.80 (1.70)	5.97 (1.81)	150.54[b]	**7.1906×10^{-53}**
WHO QoL (total)	97.45 (33.60)	102.81 (28.91)	NA	1.65[c]	0.099	NA	71.20 (28.81)	74.92 (24.86)	39.58[b]	**8.5257×10^{-17}**
Medications										
Antipsychotics, *n* (%)	NA	NA	NA	NA	NA	NA	60 (28.17)	27 (13.50)	12.51[a]	**4.032×10^{-4}**
Antidepressants, *n* (%)	NA	NA	NA	NA	NA	NA	105 (49.30)	137 (68.50)	4.23[a]	**0.040**
CPZ-equivalent (mg)	NA	NA	NA	NA	NA	358.9 (382.4)	NA	NA	NA	NA

[a]Chi-squared test. [b] *F* test. [c] *t*-test. *P* values in bold indicate statistical significance. BDI, Beck Depression Inventory; GAF:D/I, Global Assessment of Functioning Disability/Impairment Scale; GAF:S, Global Assessment of Functioning Social Scale; GF:R: Global Functioning Role Scale; GF:S, Global Functioning Social Scale; NA, not available; PANSS: positive and negative symptom scale, WHO QoL: World Health Organization quality of life.

Table 2 | Model performance of the regression analysis for the discovery model and its application to the validation, Cam-CAN and patient groups

Study group	*n*	BMIgap uncorrected (kg m^{-2})	BMIgap (kg m^{-2})	MAE (kg m^{-2})	R^2	*r*	*P*
$HC_{discovery}$	770	−0.01 (3.4)	0 (1.78)	2.75	0.28	0.53	**2.1975×10^{-56}**
$HC_{validation}$	734	1.73 (2.2)	0.23 (1.68)	2.29	0.26	0.51	**1.3696×10^{-15}**
$HC_{Cam\text{-}CAN}$	536	0.82 (0.56)	0.25 (3.26)	2.96	0.10	0.32	**7.7240×10^{-14}**
Schizophrenia	146	1.83 (3.0)	1.05 (1.53)	2.85	0.25	0.50	**1.2242×10^{-10}**
CHR	213	1.70 (3.26)	0.51 (1.68)	3.07	0.16	0.40	**2.2209×10^{-7}**
ROD	200	−0.03 (3.48)	−0.82 (1.64)	2.73	0.10	0.32	**3.7118×10^{-5}**

P values in bold indicate statistical significance (α=0.05). BMIgap is shown as the mean ± s.d. (uncorrected and corrected for BMI). Model performance metrics include the MAE, the coefficient of determination (R^2) and Pearson correlation coefficients (*r*, two-sided) between predicted and observed BMI.

The BMIgap of individuals with ROD positively correlated with both ΔW_1 (n = 141; r = 0.18, P_{FDR} = 0.053) and ΔW_2 (n = 92; r = 0.30, P_{FDR} = 0.05) at all ages and notably for young individuals aged between 15 and 20 years (ΔW_2: n = 15; r = 0.52, P_{FDR} = 0.051). Moreover, females with ROD showed a significant correlation between BMIgap and weight gain at T1 (ΔW_1: n = 70; r = 0.29, P = 0.04), while males did not (n = 71; r = 0.02, P = 0.86). CHR individuals between 25 and 40 years of age showed significant correlations between BMIgap and ΔW_1 in the +5% weight increase subgroup (n = 58; r = 0.29, P_{FDR} = 0.047) and with ΔW_2 specifically in the +3% (n = 39; r = 0.28, P_{FDR} = 0.049), +5% (n = 32; r = 0.31, P_{FDR} = 0.049) and +7% (n = 21; r = 0.27, P_{FDR} = 0.01) subgroups (Fig. 3a, Supplementary Fig. 9 and Supplementary Tables 7–10).

Weight gain predictor

The multivariate weight gain prediction model indicated a weight gain of +7% at T2 with a BAC of 59.2% (sensitivity = 64.9%, specificity = 53.5%, P < 0.05); the +3% (BAC = 52.2%; sensitivity = 52.5%, specificity = 51.9%, P = 0.21) and +5% weight gain prediction models did not perform above chance level (BAC = 45.2%, sensitivity = 62.5%, specificity = 35.2%) (Supplementary Table 4). Key predictive features for the 7% weight gain predictor included age, clinical group (ROD, CHR), exercise, somatic history, BMIgap and tobacco use. Specifically, among CHR individuals, a higher BMIgap, combined with a history of somatic conditions and reduced mindfulness-based exercises was predictive of weight gain. For individuals with ROD, BMIgap was negatively associated with 7%

https://doi.org/10.1038/s44220-025-00522-3

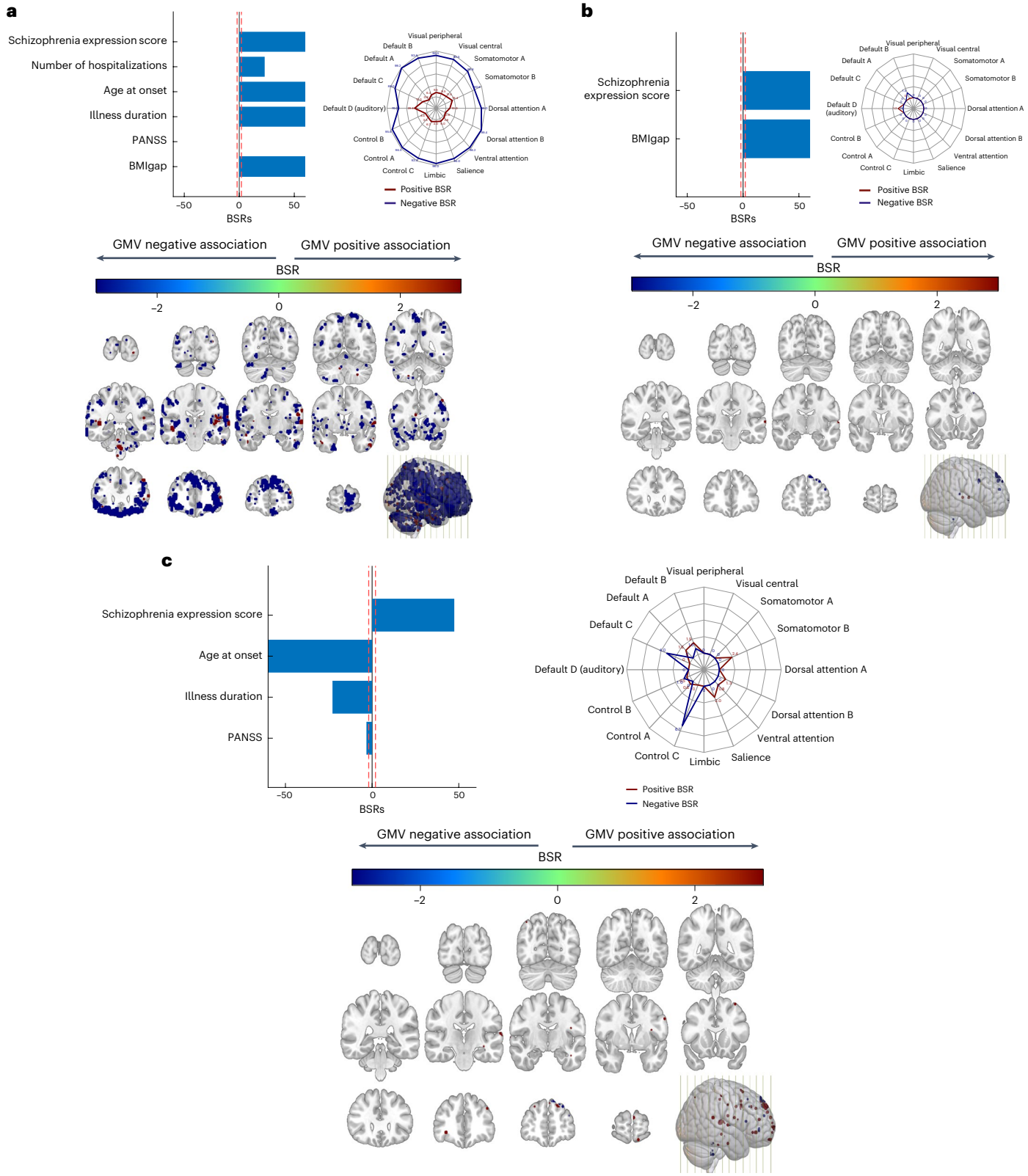

Fig. 2 | Signatures exhibiting a positive association between schizophrenia expression score and BMIgap effects. a, LV2. **b**, LV3. **c**, BMIgap-independent signature of LV5. The bar plots visualize the correlation of each variable with the LV; blue represents variables strongly contributing to the LV. The *x* axis denotes the bootstrap ratios (BSRs) on the *x* axis (interpretable as *z*-scores); the *y* axis denotes the BMIgap, schizophrenia expression score and other clinical items. The red dashed line represents a BSR of 1.96 (equivalent to a 95% CI). The contribution of individual voxels is shown using the BSR in the Montreal Neurological Institute space. Cool colors indicate voxels with a negative correlation of GMV and clinical items; warm colors represent a positive correlation. The spider plots represent the voxel contribution within the 17-network parcellation solution of the Yeo–Buckner atlas[65]. The network names and the cerebral cortical regions that compose the 17 networks are from the supplementary video in ref. 66.

https://doi.org/10.1038/s44220-025-00522-3

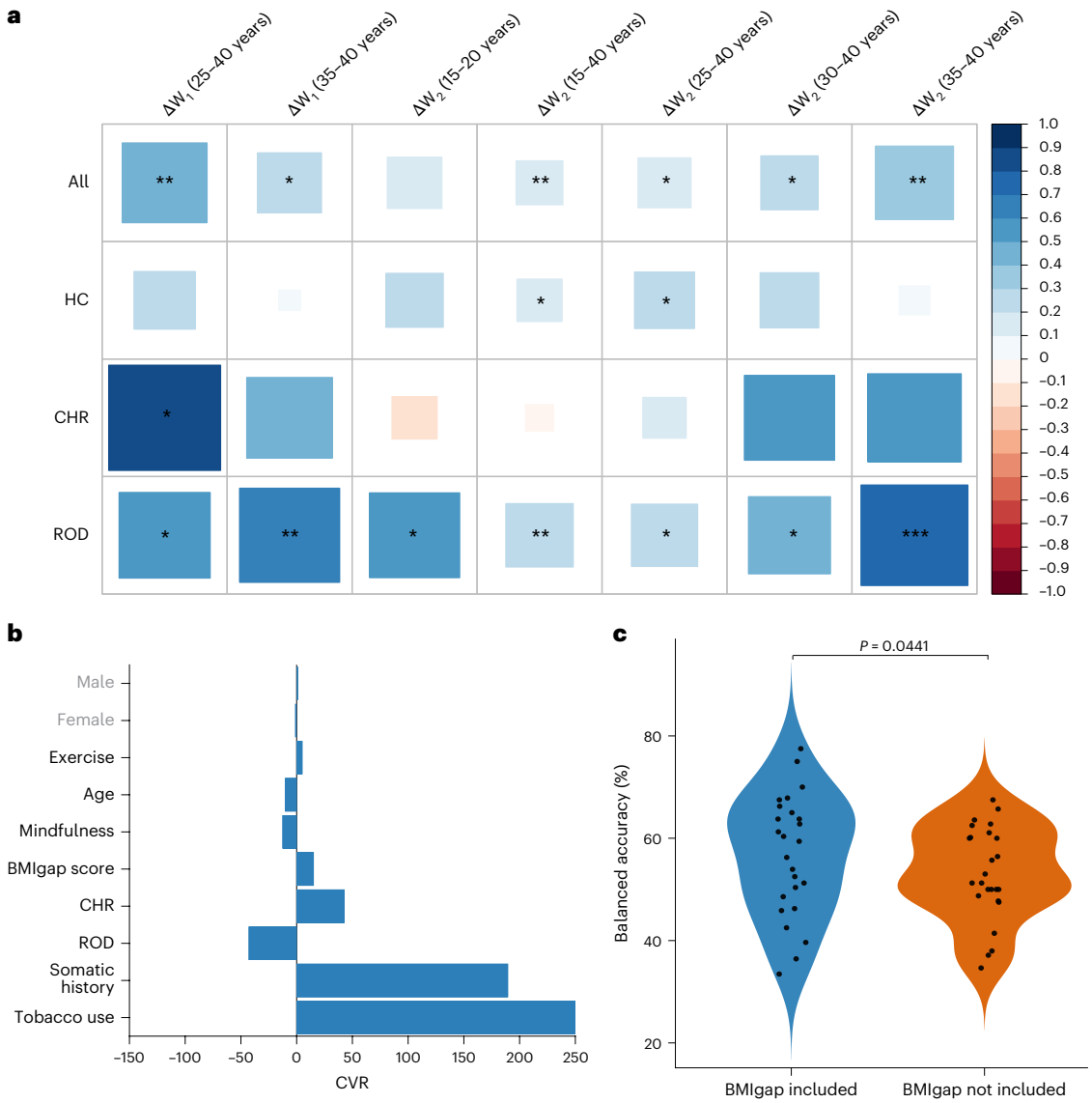

Fig. 3 | Association between BMIgap and weight change. a, Heatmap showing the correlations between BMIgap and weight change (ΔW_1 = weight$_{T1}$ − weight$_{T0}$; ΔW_2 = weight$_{T2}$ − weight$_{T0}$) across different age ranges and clinical groups (HC, CHR, ROD). Correlation coefficients were calculated using two-sided Pearson correlations. Significance was assessed with FDR correction for multiple comparisons; significant values are denoted as $^*P \le 0.05$, $^{**}P \le 0.01$ and $^{***}P \le 0.001$, with exact (FDR-adjusted) P values reported in Supplementary Tables 7–10. The plot uses blue squares to represent positive correlations and red squares for negative correlations. The size of each square corresponds to the magnitude of the correlation value, with larger squares indicating stronger correlations. **b**, Feature importance analysis for predicting 7% weight gain, expressed as the CVR. **c**, Comparison of balanced accuracy for predicting 7% weight gain at T2, with and without BMIgap as a feature. Model performance was compared using a two-sided paired t-test ($t = 1.907$, d.f. = 24, $P = 0.0441$).

weight gain, particularly in individuals with a history of lower somatic comorbidities, reduced tobacco use and older age (Fig. 3c). Notably, the predictive performance of the +7% weight reduced after excluding BMIgap as a feature (BAC = 56.1%; sensitivity = 48.6%, specificity = 63.6%; $P < 0.05$); these two models differed significantly ($P < 0.05$) (Fig. 3c).

Discussion

The aim of our study was to introduce BMIgap as a metric to evaluate BMI-related brain signatures, interrogate its overlaps with schizophrenia brain patterns and explore its implications for future weight gain.

The BMI predictor relied on lower GMV in the prefrontal and temporal regions, particularly in areas associated with reward and inhibitory control and higher GMV in the precuneus, putamen and Rolandic operculum to predict BMI. When comparing BMIgap across samples, we found no notable difference between the HC$_{discovery}$ and the independent HC$_{Cam\text{-}CAN}$ cohorts, suggesting that our model generalized well to external healthy populations. This was further supported by a notable correlation between BMI$_{predicted}$ and BMI$_{observed}$ in HC$_{Cam\text{-}CAN}$. Moreover, individuals in the psychosis spectrum (schizophrenia and CHR) showed an increased BMIgap while individuals with affective diseases (ROD) showed a decreased BMIgap. Moreover, we found that the separability of schizophrenia from HCs partly overlapped with BMI-related structural brain variation pertaining to the inhibitory control and reward systems. SPLS analysis revealed that a prefrontal-temporal brain pattern predicting both disease and BMI phenotypes was associated with longer illness, later disease onset and higher number of hospitalizations. At a group level, higher BMIgap was correlated with future weight gain, an effect particularly pronounced in the longer-term trajectories of younger individuals with depressive disorders. At an individual level, BMIgap was identified as

a predictive feature for future weight gain in combination with age, clinical group (ROD and CHR), exercise, history of somatic comorbidities and tobacco use.

The co-occurrence of higher BMI and lower GMV in the reward and salience systems in the BMI predictor model may represent a neurobiological mediator of eating behaviors[16–19]. Furthermore, BMI-predictive GMV reductions in brain areas related to taste, reward and inhibitory control, may contribute to increased susceptibility to hypercaloric eating[17,19]. These GMV alterations align with dysfunctional reward anticipation and impaired inhibitory control, which have been implicated in heightened food cravings, compulsive eating patterns and reduced sensitivity to homeostatic satiety signals[17,19]. Additionally, given the overlap between the BMI-predictive and schizophrenia signatures within inhibitory, reward and cognitive control regions, this suggests an underlying neural vulnerability between obesity and schizophrenia that is consistent with previous research[20,23]. Our findings substantiate previous reports that prefrontal deficits might lead to reduced cognitive control and may therefore amplify the risk of addictive behaviors, such as overeating, which could substantially contribute to an increased BMI in psychiatric patients[17,18,23]. We did not observe notable differences between $HC_{discovery}$ and $HC_{Cam\text{-}CAN;}$ $BMI_{predicted}$ and $BMI_{observed}$ for $HC_{Cam\text{-}CAN}$ strongly correlated, suggesting that our model generalized well across independent HC samples. When applied to clinical groups, we observed a positive BMIgap for the schizophrenia and CHR groups and a negative BMIgap for the group with ROD compared with the $HC_{discovery}$. The positive BMIgap in schizophrenia and CHR suggests that these groups exhibit brain structural patterns typically associated with HCs who have a higher BMI, despite having lower actual BMI than predicted. This may reflect underlying pathophysiological processes, such as neuroinflammation, insulin resistance or gut–brain axis disruptions, which are known to affect both metabolic regulation and brain structure[31]. In schizophrenia, these effects may be more pronounced than in CHR because of longer illness duration and associated metabolic burden, potentially predisposing individuals to future weight gain. Conversely, the group with ROD group a negative BMIgap, indicating that their brain structural patterns more closely resemble those of HCs with a lower BMI, despite having higher actual BMI than predicted. This finding may relate to early-stage depressive phenotypes, often characterized by appetite suppression and reduced energy intake, and may reflect a distinct neurobiological profile in depression compared to psychotic disorders. These interpretations align with prior evidence linking early or untreated depression to reduced appetite, weight loss, altered energy metabolism, and abnormal hypothalamic–pituitary–adrenal signaling in patients with comorbid depression and anorexia nervosa[32–34]. The significance of BMIgap lies in its ability to capture systematic brain-based alterations in BMI prediction across different psychiatric populations, highlighting distinct patterns of brain–metabolism interactions that may not be fully explained by traditional anthropometric measures such as BMI.

Importantly, our analyses suggest that BMIgap is largely unaffected by the intake of weight-gain versus weight-neutral medication, indicating that brain-based BMI deviations may reflect more stable neurobiological traits rather than being predominantly driven by pharmacological effects. This further supports the utility of BMIgap as a potential tool of brain–metabolic alterations, independent of current medication status. Nonetheless, future studies with larger samples and longitudinal designs are needed to explore potential medication-related changes in brain-based BMI predictions over time.

Moreover, occurrence of metabolic syndromes in psychiatric patients is often linked to psychiatric medication, namely antipsychotics and antidepressants[11,35,36]. Antipsychotics affect the mesolimbic dopaminergic system and the ventromedial nucleus, thereby altering behavioral responses to environmental stimuli and regulating both food intake and body weight[35]. Antidepressants affect metabolic risk by increasing appetite and suppressing satiety, primarily through histaminergic and serotonin receptor antagonism[11,12]. However, we did not find notable differences when comparing the BMIgap of fully naive, partly naive and concurrently antidepressant-antipsychotic-treated CHR or ROD. Moreover, we did not observe any clear associations between BMIgap and antipsychotic dosage in patients with schizophrenia. These findings indicate that BMIgap captures a neurobiological BMI signature, which may represent a more disease-specific or individual predisposition toward future weight changes. This finding aligns with previous research indicating that patients with psychiatric disorders are at an increased risk of developing metabolic syndrome and obesity, independent of medication use[37,38], contrasting other literature that primarily attributes weight gain to the effects of psychiatric medication[11,12].

The phenotypic association analysis linked control and reward brain networks to schizophrenia diagnosis, BMIgap and clinical variables in unique ways. The multivariate signatures of concurrently high BMIgap and schizophrenia expression scores (LV2, LV3) were associated with both a decrease in GMV within the limbic network and increased GMV within the DMN (auditory) network. In obesity research, these networks have been involved in reward processing[39], food motivation[40] and executive and affective control[41]; in schizophrenia research, they have been particularly implicated in the impaired processing of negative emotions[42]. Furthermore, later disease onset, higher hospitalization frequency and longer illness, were associated with both higher BMIgap and schizophrenia expression scores, thereby implying a potential association between the severity of schizophrenia and the presence of obesity risk traits. Moreover, we identified a pattern independent of BMIgap (LV5) suggesting that there are distinct effects of schizophrenia and BMI on the brain, indicating that those with early onset, shorter illness and milder symptoms are less likely to show high schizophrenia diagnostic separability, thus highlighting the complexity of schizophrenia subtypes and the variability in its manifestation and progression.

Moreover, our assertion that BMIgap is associated with future weight changes was supported by the positive correlation between BMIgap and future weight change observed across all groups, with the strength of this correlation increasing from the 1-year to the 2-year follow-ups. Notably, these correlations were most pronounced among young individuals (15–20 years) in the group with ROD and young adults (25–40 years) in the CHR group, indicating that individuals in the early stages of psychiatric illness may exhibit distinct brain signatures that predispose them to future weight gain. Furthermore, the 7% weight gain predictor highlighted that young adults with ROD who have higher exercise rates, use less tobacco, have less somatic comorbidities and lower BMIgap are less likely to experience weight gain. Conversely, younger CHR individuals with reduced exercise rates, more history of somatic comorbidities, higher tobacco use and higher BMIgap were at an increased risk for future weight gain. Notably, exclusion of the BMIgap feature from the 7% weight gain predictor led to a marked reduction in predictive accuracy of the model in correctly predicting future weight gain.

The translational value of BMIgap lies in its potential to identify individuals at risk for future weight changes, especially weight gain, in early disease stages, and particularly in vulnerable, at-risk populations such as CHR individuals and individuals with ROD. Assessing BMIgap could potentially enable identification of individuals who, despite having a BMI in the normal range, are in fact, neurobiologically, at increased risk for future weight gain. This could lead to stratified, targeted and timely interventions, such as early access to guided physical exercise or add-on medication such as metformin[43,44]. More specifically, given its association with reward and inhibitory control networks, patients with a high BMIgap may benefit from targeted psychotherapy aimed at enhancing self-regulation, impulse control and reward sensitivity, which are key factors influencing eating behavior and metabolic health[41]. Approaches such as cognitive

behavioral therapy and inhibitory control training enhance executive function, decision-making and impulse control in relation to food intake[41,45]. Additionally, dopaminergic modulation may help regulate reward processing and compulsive eating behaviors, particularly in individuals exhibiting heightened reward sensitivity to hypercaloric foods[46]. All of this would eventually be aimed at preventing weight gain and associated metabolic syndromes in at-risk individuals and thus improve treatment adherence, overall quality of life and treatment outcomes[29,30].

Limitations

One limitation of our study is the lack of individuals with very high (>35 kg m^{-2}) or low (<18 kg m^{-2}) BMI, which limits the generalizability of our findings to patients with comorbidities related to overweight (for example, type 2 diabetes, hypertension) or underweight (for example, anorexia). The absence of harmonized clinical and longitudinal data across cohorts, particularly the lack of weight follow-up data in the group with schizophrenia, limited our ability to assess BMIgap's association with future weight changes in this population. More broadly, the lack of standardized clinical and medication data is a common limitation in multisite studies[47–49]. Future research could address these challenges by systematically collecting metabolic, medication-related and clinical factors influencing brain structure and psychiatric conditions. Such efforts should extend to early-stage populations, including CHR and ROD, as well as a broader range of psychiatric disorders, such as posttraumatic stress disorder and obsessive–compulsive disorder. Furthermore, our study did not include metabolic markers such as lipid profiles, fasting glucose or homeostatic model assessment for insulin resistance, nor precise obesity measures like waist-to-hip ratio and body fat percentage. While BMI provided a practical and widely used index for this endeavor, future research incorporating a wider, potentially more comprehensive array of metabolic and anthropometric markers is warranted to deepen our insights into brain–metabolism interactions in psychiatric populations[16–18,50]. Finally, pubertal status was not assessed in the 15–20-year-old subgroup, which may have influenced weight-related trajectories and represents a limitation of the current analysis.

Conclusion

In conclusion, our study identified BMIgap as a crucial metric for exploring the relationship between BMI and brain structure in psychiatric populations, particularly within the depression and schizophrenia spectrum. We found that elevated BMIgap was associated with pronounced neurobiological alterations in reward and inhibitory control systems, indicating a complex interplay between obesity and schizophrenia. Our findings further suggest that BMIgap could potentially be a predictive indicator of future weight gain, especially among younger individuals with a higher disease burden. Therefore, BMIgap could serve as a template for machine learning and brain imaging to enhance the early identification of patients at risk for metabolic complications. Integrating BMIgap, or future, more sophisticated tools, into clinical assessments may improve strategies for preventing weight gain in psychiatric patients.

Methods

Sample

The study followed the Transparent Reporting of a Multivariable Prediction Model for Individual Prognosis or Diagnosis reporting guidelines (www.equator-network.org/reporting-guidelines/tripod-statement/). We included T1-weighted magnetic resonance imaging (MRI) scans of 1,504 HCs ($HC_{discovery}$: n = 770, age = 41.3 ± 15.5 years, 56.5% female; $HC_{validation}$: n = 734, age = 32.2 ± 12.8 years, 50.8% female; $HC_{Cam\text{-}CAN}$: n = 536, age = 54.3 ± 18.6 years, 48.7% female) from five independent datasets covering 15 sites: Information eXtraction from Images (IXI) (https://brain-development.org/ixi-dataset/); Personalized Prognostic Tools for Early Psychosis Management (PRONIA) (www.pronia.eu); the Norwegian Centre for Mental Disorders Research (NORMENT) (www.med.uio.no/norment/)[51]; the Munich Brain Imaging Database (MUC[52]); and the Cambridge Centre for Ageing and Neuroscience (Cam-CAN[53,54]) datasets (Supplementary Methods). Moreover, three patient populations were included: individuals with schizophrenia (n = 146, age = 30.8 ± 10.0 years, 23.3% female) from the MUC cohort and CHR (n = 213, age = 23.9 ± 5.2 years, 48.4% female) and individuals with ROD (n = 200, age = 26.0 ± 6.4 years, 48.0% female) from the PRONIA study (Table 1 and Supplementary Table 2). All participants gave informed consent and received compensation. All studies were approved by their local ethics committee and adhered to the ethical standards outlined in the Declaration of Helsinki[55]. All datasets were collected in collaboration with local research teams, who contributed to study design, implementation and authorship, ensuring compliance with local ethical standards and relevance.

Modeling framework

In our study, we developed an individualized BMI prediction model based on voxel-wise GMV. This strategy builds on previous work by Opel et al.[18], who applied multivariate models to predict BMI from GMV in HCs[18]. We extended this approach by implementing a normative modeling framework that not only enables individualized predictions but also quantifies individualized deviations from expected, that is, 'normative', brain–BMI relationships. This allowed us to derive a brain-based vulnerability measure, BMIgap, which captures how much an individual's brain structure deviates from typical BMI-related patterns. We then applied this model to clinical populations to investigate brain-based metabolic vulnerability across different psychiatric conditions. A detailed explanation of our modeling framework and sample selection procedure is provided in the (Supplementary Methods).

Participant selection

We included HCs aged 15–75 years with a BMI range of 18.5–35 kg m^{-2} without current or previous psychiatric disorders in the discovery model by following these steps: (1) to avoid an underrepresentation of the tails of the BMI distribution and to maximize model generalizability throughout the investigated BMI range, we selected 770 HCs from a sample of 1,504 HCs and distributed them into 33 BMI bins (0.5 BMI per bin) from the 18.5–20.0 bin to the 34.5–35.0 bin, aiming for an equal number of individuals per bin to reduce bias toward the overrepresented normal BMI range and improving generalizability to individuals with high or low BMI (Supplementary Fig. 1a); (2) to control for the natural correlation between BMI and age, age distribution was matched in each BMI bin wherever possible, so that in addition to equal numbers of individuals across the BMI range, the 33 BMI bins had a comparable mean age[56] (Supplementary Fig. 1c). These 770 HCs constituted the $HC_{discovery}$ sample; the remaining 734 HCs constituted the $HC_{validation}$ sample, while 536 HC individuals from the Cam-CAN dataset ($HC_{Cam\text{-}CAN}$) constituted an additional external validation sample for our model. The clinical population consisted of individuals with schizophrenia (n = 146), CHR (n = 213) and ROD (n = 200) (Supplementary Figs. 1 and 2 and Supplementary Methods).

MRI data acquisition and preprocessing

Participants in the IXI and PRONIA studies underwent MRI scanning at 1.5T or 3T, while NORMENT, Cam-CAN and MUC participants were examined with 1.5T MRI scanners (Supplementary Methods and Supplementary Table 1). To facilitate between-study comparability, we applied the VBM8 preprocessing pipeline described in ref. 18 to produce normalized, modulated GMV tissue maps (Supplementary Methods). For computational efficiency and noise reduction, GMV images were resliced to a 3 × 3 × 3-mm^3 isotropic voxel resolution.

Machine learning analysis

The open-source machine learning software NeuroMiner (v1.1) (https://github.com/neurominer-git/NeuroMiner_1.1) was used for the training and application of all supervised machine learning models. To prevent information leakage between training and test data, thereby limiting overfitting risk and enhancing model generalizability, we implemented a repeated nested cross-validation with five folds and five permutations each on the inner and outer cross-validation cycles. All preprocessing parameters were computed using the training data of the inner cross-validation cycle and applied to the data of the inner test and outer validation folds. Voxel-wise GMV data preprocessing included: (1) Gaussian smoothing with 0-mm, 3-mm, 6-mm and 9-mm full-width at half-maximum kernel widths; (2) regressing out age effects using partial correlation analysis; (3) mean offset correction to remove site effects, that is, scanner effects; (4) principal component analysis with different energy levels (0.25, 0.50, 0.75) to reduce the dimensionality of the image space; and (5) voxel-wise scaling from 0 to 1. The models were then trained on the inner training folds and applied to the inner test and outer validation folds, ensuring that validation remained completely independent of training. We used *v*-support vector machine regression with a linear kernel to predict BMI based on whole-brain voxel-wise GMV (71,276 features) using the MAE as the optimization criterion. The statistical significance of the model was evaluated using 1,000 permutations of the BMI label (significance level $\alpha = 0.05$). Predictive brain patterns were visualized at the voxel level combining the grand means of the CVR[57] and sign-based consistency mapping, thereby assessing whether a feature consistently predicted higher or lower BMI across cross-validation partitions[58] (Supplementary Methods). We applied this BMI predictor to the $HC_{validation}$ and $HC_{Cam\text{-}CAN}$ cohorts to assess the model's generalizability. Furthermore, the BMI predictor was applied to individuals with schizophrenia, ROD and CHR to obtain brain-based BMI predictions for these clinical populations.

BMIgap calculation

BMIgap was calculated by subtracting the measured BMI from the brain-based predicted BMI ($BMIgap = BMI_{predicted} - BMI_{measured}$). A positive BMIgap indicates that an individual's brain structure resembles that of someone with a higher BMI than their actual BMI measurement, whereas a negative BMIgap suggests the opposite. To assess systematic deviations within groups, we compared BMIgap values across diagnostic categories (HC, schizophrenia, ROD, CHR), allowing us to quantify whether specific populations consistently exhibit overestimations or underestimations in brain-based BMI relative to the reference sample. To mitigate systematic bias in predicted BMI, characterized by overestimation at lower BMI ranges and underestimation at higher BMI ranges, BMIgap was adjusted for BMI using partial correlation analysis[59] (Supplementary Methods and Supplementary Figs. 3 and 4). We used the corrected BMIgap for all further analysis steps. Furthermore, to investigate potential medication effects on BMIgap, we conducted additional analyses. First, we independently calculated BMIgap for antipsychotic-naive and antidepressant-naive individuals with CHR and ROD to investigate whether medication influenced BMIgap in these subpopulations. Next, we categorized individuals in the CHR and ROD groups based on whether they were receiving weight-gain-associated medications (for example, mirtazapine, olanzapine, clozapine, quetiapine, chlorpromazine) or weight-neutral medications (for example, bupropion, lurasidone, ziprasidone) at baseline and compared BMIgap values across these subgroups[43,44]. As there were no unmedicated patients with schizophrenia, we correlated BMIgap with their chlorpromazine equivalents.

Clinical investigation of BMIgap

To understand the clinical implications of BMIgap, we analyzed its relationship with clinical variables, particularly within the group with schizophrenia. To identify brain patterns distinguishing individuals with schizophrenia from HCs, we trained a schizophrenia ($n = 146$) versus $HC_{discovery}$ classifier in the MUC sample ($n = 133$), using the same preprocessing and cross-validation settings as the BMI prediction model. This classification allowed us to assess whether BMI-predictive GMV regions overlap with GMV regions distinguishing individuals with schizophrenia from HCs, indicating potential shared neuroanatomical substrates.

The binarized sign-consistency maps derived from the schizophrenia and BMI predictors were overlapped to identify brain regions commonly predictive of both phenotypes (Supplementary Methods). Furthermore, we extracted the decision scores from the schizophrenia classifier, which we refer to as the schizophrenia expression score. A higher schizophrenia expression score indicates a higher likelihood to be classified as having schizophrenia and therefore a greater neuroanatomical similarity to schizophrenia, while a lower schizophrenia expression score reflects higher likelihood of HC classification and neuroanatomical HC similarity.

Next, we studied the covariation between BMIgap, schizophrenia expression and clinical variables within the overlapping brain regions of schizophrenia and BMI. To this end, we used multivariate SPLS using the SPLS Toolbox described in refs. 60,61 to investigate the covariance patterns between two data domains in the schizophrenia sample: (1) a six-feature matrix, including BMIgap, schizophrenia expression scores, PANSS total score, age at onset, illness duration and number of hospitalizations; and (2) a brain data matrix containing the vectorized voxels extracted using the binarized mask of overlapping BMI-predictive and schizophrenia-predictive voxels. The SPLS algorithm uses singular value decomposition to generate multiple layers of distinct, multivariate associative effects between the two data matrices, called LVs (Supplementary Methods).

Investigation of BMIgap and future weight change

We investigated the association between BMIgap and future weight change using two approaches: (1) correlation analysis; and (2) machine learning-based prediction of weight gain. In the PRONIA cohort, where longitudinal data were available, we correlated BMIgap to weight changes at the 1-year (T1) and 2-year (T2) follow-ups. Weight changes were calculated as the difference between the weight at the follow-up time point and the weight at baseline (T0): 1 year ($\Delta W_1 = weight_{T1} - weight_{T0}$); 2 years ($\Delta W_2 = weight_{T2} - weight_{T0}$). The same age range stratifications were applied consistently across both time points to ensure comparability in our analyses. Correlation analyses were conducted for the entire cohort, and separately for sex and study group. In the first step, we analyzed the correlation between BMIgap and all observed weight changes. Building on the previous literature, we correlated BMIgap to weight changes only within subpopulations of patients who exhibited at least a +3%, +5% or +7% weight gain at the respective follow-up[62–64]. Additionally, to examine potential age-related effects, we analyzed these correlations across several age ranges, including broader spans (15–40, 20–40, 25–40, 30–40 and 35–40 years) and finer-grained 5-year intervals (15–20, 20–25, 25–30, 30–35 and 35–40 years). Finally, we used the three weight gain thresholds (+3%, +5% and +7%) as classification criteria to predict whether individuals with CHR and ROD experienced weight gain above these thresholds at T1 and T2 or not. We used BMIgap as well as age, sex, study group (ROD, CHR), exercise (strenuous exercise or mindfulness activities such as yoga and meditation) and history of somatic comorbidities (that is, whether the individual suffered from somatic illness) as features. Classification analyses were conducted with and without BMIgap as a feature to assess if BMIgap significantly affects the prediction of future weight gain ($P < 0.05$).

Reporting summary

Further information on research design is available in the Nature Portfolio Reporting Summary linked to this article.

Data availability

Parts of the data, including the IXI dataset (https://brain-development.org/ixi-dataset/) and the CAM-CAN dataset (https://camcan-archive.mrc-cbu.cam.ac.uk), are accessible to researchers upon request from the respective repositories. Other datasets (PRONIA, MUC, NORMENT) analyzed during the current study are not publicly available because of data sharing restrictions defined in the participants' signed informed consent agreements. Trained models are available from the corresponding author upon reasonable request.

Code availability

The code supporting the findings of this study is available via GitHub at https://github.com/adyasha95/BMIgapCodeRepo.

References

1. *Surveillance of Chronic Disease Risk Factors: Country Level Data and Comparable Estimates* (WHO, 2005); https://iris.who.int/handle/10665/43190
2. Heymsfield, S. B. & Wadden, T. A. Mechanisms, pathophysiology, and management of obesity. *N. Engl. J. Med.* **376**, 1492 (2017).
3. Weiss, F. et al. Psychiatric aspects of obesity: a narrative review of pathophysiology and psychopathology. *J. Clin. Med.* **9**, 2344 (2020).
4. Khafagy, R. & Dash, S. Obesity and cardiovascular disease: the emerging role of inflammation. *Front. Cardiovasc. Med.* **8**, 768119 (2021).
5. Rajan, T. & Menon, V. Psychiatric disorders and obesity: a review of association studies. *J. Postgrad. Med.* **63**, 182–190 (2017).
6. Afzal, M. et al. Prevalence of overweight and obesity in people with severe mental illness: systematic review and meta-analysis. *Front. Endocrinol.* **12**, 769309 (2021).
7. Abdullah, H. M., Shahul, H. A., Hwang, M. Y. & Ferrando, S. Comorbidity in schizophrenia: conceptual issues and clinical management. *Focus (Am. Psychiatr. Pub.)* **18**, 386–390 (2020).
8. De Micheli, A. et al. Physical health and transition to psychosis in people at clinical high risk. *Biomedicines* **12**, 523 (2024).
9. Kar, N. & Barreto, S. Influence of lifestyle factors on metabolic syndrome in psychiatric patients attending a community mental health setting: a cross-sectional study. *Indian J. Psychol. Med.* **46**, 313–322 (2024).
10. Sadeghirad, B., Duhaney, T., Motaghipisheh, S., Campbell, N. R. C. & Johnston, B. C. Influence of unhealthy food and beverage marketing on children's dietary intake and preference: a systematic review and meta-analysis of randomized trials. *Obes. Rev.* **17**, 945–959 (2016).
11. Gill, H. et al. Antidepressant medications and weight change: a narrative review. *Obesity* **28**, 2064–2072 (2020).
12. Serretti, A. & Mandelli, L. Antidepressants and body weight: a comprehensive review and meta-analysis. *J. Clin. Psychiatry* **71**, 1259–1272 (2010).
13. Hryhorczuk, C., Sharma, S. & Fulton, S. E. Metabolic disturbances connecting obesity and depression. *Front. Neurosci.* **7**, 177 (2013).
14. Sarwer, D. B. & Polonsky, H. M. The psychosocial burden of obesity. *Endocrinol. Metab. Clin. North Am.* **45**, 677–688 (2016).
15. Lee, K., Akinola, A. & Abraham, S. Antipsychotic-induced weight gain: exploring the role of psychiatrists in managing patients' physical health—challenges, current options and direction for future care. *BJPsych Bull.* **48**, 24–29 (2024).
16. Li, L. et al. Gray matter volume alterations in subjects with overweight and obesity: evidence from a voxel-based meta-analysis. *Front. Psychiatry* **13**, 955741 (2022).
17. Fernández-Andújar, M., Morales-García, E. & García-Casares, N. Obesity and gray matter volume assessed by neuroimaging: a systematic review. *Brain Sci.* **11**, 999 (2021).
18. Opel, N. et al. Prefrontal gray matter volume mediates genetic risks for obesity. *Mol. Psychiatry* **22**, 703–710 (2017).
19. Stice, E., Figlewicz, D. P., Gosnell, B. A., Levine, A. S. & Pratt, W. E. The contribution of brain reward circuits to the obesity epidemic. *Neurosci. Biobehav. Rev.* **37**, 2047–2058 (2013).
20. Tsai, S.-Y. et al. Body mass index, residual psychotic symptoms, and inflammation associated with brain volume reduction in older patients with schizophrenia. *Int. J. Geriatr. Psychiatry* **35**, 728–736 (2020).
21. Opel, N. et al. Brain structural abnormalities in obesity: relation to age, genetic risk, and common psychiatric disorders. *Mol. Psychiatry* **26**, 4839–4852 (2021).
22. Leutner, M. et al. Obesity as pleiotropic risk state for metabolic and mental health throughout life. *Transl. Psychiatry* **13**, 175 (2023).
23. McWhinney, S. R. et al. Obesity and brain structure in schizophrenia—ENIGMA study in 3021 individuals. *Mol. Psychiatry* **27**, 3731–3737 (2022).
24. McWhinney, S. et al. Obesity as a risk factor for accelerated brain ageing in first-episode psychosis—a longitudinal study. *Schizophr. Bull.* **47**, 1772–1781 (2021).
25. De Hert, M., Schreurs, V., Vancampfort, D. & Van Winkel, R. Metabolic syndrome in people with schizophrenia: a review. *World Psychiatry* **8**, 15–22 (2009).
26. Peritogiannis, V., Ninou, A. & Samakouri, M. Mortality in schizophrenia-spectrum disorders: recent advances in understanding and management. *Healthcare* **10**, 2366 (2022).
27. Hinchliffe, N., Capehorn, M. S., Bewick, M. & Feenie, J. The potential role of digital health in obesity care. *Adv. Ther.* **39**, 4397–4412 (2022).
28. Bays, H. E. et al. Artificial intelligence and obesity management: an Obesity Medicine Association (OMA) Clinical Practice Statement (CPS) 2023. *Obes. Pillars* **6**, 100065 (2023).
29. Tian, Y. E. et al. Evaluation of brain–body health in individuals with common neuropsychiatric disorders. *JAMA Psychiatry* **80**, 567–576 (2023).
30. Alhindi, Y. A., Khalifa, N., Al-Khyatt, W. & Idris, I. The use of non-invasive brain stimulation techniques to reduce body weight and food cravings: a systematic review and meta-analysis. *Clin. Obes.* **13**, e12611 (2023).
31. Phelps, N. H. et al. Worldwide trends in underweight and obesity from 1990 to 2022: a pooled analysis of 3663 population-representative studies with 222 million children, adolescents, and adults. *Lancet* **403**, 1027–1050 (2024).
32. Bohon, C. & Welch, H. Quadratic relations of BMI with depression and brain volume in children: analysis of data from the ABCD study. *J. Psychiatr. Res.* **136**, 421–427 (2021).
33. Baothman, O. A., Zamzami, M. A., Taher, I., Abubaker, J. & Abu-Farha, M. The role of gut microbiota in the development of obesity and diabetes. *Lipids Health Dis.* **15**, 108 (2016).
34. Wu, H. et al. Schizophrenia and obesity: May the gut microbiota serve as a link for the pathogenesis? *iMeta* **2**, e99 (2023).
35. Panariello, F., De Luca, V. & de Bartolomeis, A. Weight gain, schizophrenia and antipsychotics: new findings from animal model and pharmacogenomic studies. *Schizophr. Res. Treat.* **2011**, 459284 (2011).
36. Fava, M. Weight gain and antidepressants. *J. Clin. Psychiatry* **61**, 37–41 (2000).
37. Ferns, G. Cause, consequence or coincidence: the relationship between psychiatric disease and metabolic syndrome. *Transl. Metab. Syndr. Res.* **1**, 23–38 (2018).
38. Penninx, B. W. J. H. & Lange, S. M. M. Metabolic syndrome in psychiatric patients: overview, mechanisms, and implications. *Dialogues Clin. Neurosci.* **20**, 63–73 (2018).
39. Avery, J. A. et al. Obesity is associated with altered mid-insula functional connectivity to limbic regions underlying appetitive responses to foods. *J. Psychopharmacol.* **31**, 1475–1484 (2017).

40. Dugré, J. R., Bitar, N., Dumais, A. & Potvin, S. Limbic hyperactivity in response to emotionally neutral stimuli in schizophrenia: a neuroimaging meta-analysis of the hypervigilant mind. *Am. J. Psychiatry* **176**, 1021–1029 (2019).
41. Stoeckel, L. E. et al. Psychological and neural contributions to appetite self-regulation. *Obesity***25**, S17–S25 (2017).
42. Tamminga, C. A. et al. Limbic system abnormalities identified in schizophrenia using positron emission tomography with fluorodeoxyglucose and neocortical alterations with deficit syndrome. *Arch. Gen. Psychiatry* **49**, 522–530 (1992).
43. Dayabandara, M. et al. Antipsychotic-associated weight gain: management strategies and impact on treatment adherence. *Neuropsychiatr. Dis. Treat.* **13**, 2231–2241 (2017).
44. Hakami, A. Y. et al. The association between antipsychotics and weight gain and the potential role of metformin concomitant use: a retrospective cohort study. *Front. Psychiatry* **13**, 914165 (2022).
45. Pasquale, E. K., Boyar, A. M. & Boutelle, K. N. Reward and inhibitory control as mechanisms and treatment targets for binge eating disorder. *Curr. Psychiatry Rep.* **26**, 616–625 (2024).
46. Stover, P. J. et al. Neurobiology of eating behavior, nutrition, and health. *J. Intern. Med.* **294**, 582–604 (2023).
47. Dinsdale, N. K. et al. Challenges for machine learning in clinical translation of big data imaging studies. *Neuron* **110**, 3866–3881 (2022).
48. Kahn, M. G., Raebel, M. A., Glanz, J. M., Riedlinger, K. & Steiner, J. F. A pragmatic framework for single-site and multisite data quality assessment in electronic health record-based clinical research. *Med. Care* **50**, S21–S29 (2012).
49. Lock, J. et al. Challenges in conducting a multi-site randomized clinical trial comparing treatments for adolescent anorexia nervosa. *Int. J. Eat. Disord.* **45**, 202–213 (2012).
50. Herrmann, M. J., Tesar, A.-K., Beier, J., Berg, M. & Warrings, B. Grey matter alterations in obesity: a meta-analysis of whole-brain stÿudies. *Obes. Rev.* **20**, 464–471 (2019).
51. Wolfers, T. et al. Mapping the heterogeneous phenotype of schizophrenia and bipolar disorder using normative models. *JAMA Psychiatry* **75**, 1146–1155 (2018).
52. Koutsouleris, N. et al. Individualized differential diagnosis of schizophrenia and mood disorders using neuroanatomical biomarkers. *Brain* **138**, 2059–2073 (2015).
53. Taylor, J. R. et al. The Cambridge Centre for Ageing and Neuroscience (Cam-CAN) data repository: structural and functional MRI, MEG, and cognitive data from a cross-sectional adult lifespan sample. *Neuroimage* **144**, 262–269 (2017).
54. Shafto, M. A. et al. The Cambridge Centre for Ageing and Neuroscience (Cam-CAN) study protocol: a cross-sectional, lifespan, multidisciplinary examination of healthy cognitive ageing. *BMC Neurol.* **14**, 204 (2014).
55. Goodyear, M. D. E., Krleza-Jeric, K. & Lemmens, T. The Declaration of Helsinki. *BMJ* **335**, 624–625 (2007).
56. Stevens, J. et al. The effect of age on the association between body-mass index and mortality. *N. Engl. J. Med.* **338**, 1–7 (1998).
57. Koutsouleris, N. et al. Prediction models of functional outcomes for individuals in the clinical high-risk state for psychosis or with recent-onset depression: a multimodal, multisite machine learning analysis. *JAMA Psychiatry* **75**, 1156–1172 (2018).
58. Gómez-Verdejo, V., Parrado-Hernández, E., Tohka, J. & Alzheimer's Disease Neuroimaging Initiative. Sign-consistency based variable importance for machine learning in brain imaging. *Neuroinformatics* **17**, 593–609 (2019).
59. Zhang, B., Zhang, S., Feng, J. & Zhang, S. Age-level bias correction in brain age prediction. *Neuroimage Clin.* **37**, 103319 (2023).
60. Monteiro, J. M., Rao, A., Shawe-Taylor, J. & Mourão-Miranda, J. A multiple hold-out framework for Sparse Partial Least Squares. *J. Neurosci. Methods* **271**, 182–194 (2016).
61. Popovic, D. et al. Traces of trauma: a multivariate pattern analysis of childhood trauma, brain structure, and clinical phenotypes. *Biol. Psychiatry* **88**, 829–842 (2020).
62. De Hert, M. et al. Cardiovascular disease and diabetes in people with severe mental illness position statement from the European Psychiatric Association (EPA), supported by the European Association for the Study of Diabetes (EASD) and the European Society of Cardiology (ESC). *Eur. Psychiatry* **24**, 412–424 (2009).
63. Svärd, A. et al. Weight change among normal weight, overweight and obese employees and subsequent diagnosis-specific sickness absence: a register-linked follow-up study. *Scand. J. Public Health* **48**, 155–163 (2020).
64. Eder, J. et al. Who is at risk for weight gain after weight-gain associated treatment with antipsychotics, antidepressants, and mood stabilizers: a machine learning approach. *Acta Psychiatr. Scand.* **151**, 231–244 (2024).
65. Yeo, B. T. et al. The organization of the human cerebral cortex estimated by intrinsic functional connectivity. *J. Neurophysiol.* **106**, 1125–1165 (2011).
66. Baker, J. T., et al. Disruption of cortical association networks in schizophrenia and psychotic bipolar disorder. *JAMA Psychiatry* **71**, 109–118 (2014).

Acknowledgements

We thank S. Miedl for helping with the administrative work. This study was supported by the German Federal Ministry of Education and Research (01ZX1904E and 01ZX2204A) as a part of the COMorbidity Modeling via Integrative Transfer machine learning in MENTal illness project. PRONIA is a collaboration project funded by the European Union under the 7th Framework Programme (grant no. 602152). N.K. is supported through grants from the National Institutes of Health (U01MH124639-01; ProNET), the Wellcome Trust, the German Innovation Fund (CARE project), the German Federal Ministry of Education and Research (COMMITMENT and BEST projects), as well as ERA PerMed (IMPLEMENT project). A.K. is funded through the COMMITMENT project. D.P. was supported by the Else-Kröner-Fresenius-Foundation through the Clinician Scientist Program 'EKFS-Translational Psychiatry'. E. Schwarz is supported through grants from the German Federal Ministry of Education and Research (COMMITMENT, grant no. 01ZX2204A), BEST (grant no. 01EK2101B) and IMPLEMENT (grant no. 01KU1905A)). The Norwegian study group is funded by the Research Council of Norway and the KG Jebsen Foundation. The funders were not involved in the design and conduct of the study; the collection, management, analysis and interpretation of the data; the preparation, review or approval of the manuscript; and the decision to submit the manuscript for publication.

Author contributions

A.K., A.W. and N.K. had access to all the study data. N.K. and E. Schwarz conceived and designed the study. A.K., D.P., A.W. and N.K. were responsible for the analytical framework and data interpretation. A.K. was responsible for data organization. M.L.P. provided the NORMENT data. N.K., J.K., R.K.R.S., J.H., R.L., A.B., P.B., R.U., S.B., S.J.W., R.L., P.F., L.T.W., O.A.A. and E.M. were responsible for data collection. A.K., A.W., D.P. and E. Sarisik were responsible for the analysis setup. A.K. wrote the first manuscript draft, which was critically revised by D.P., A.W. and N.K. E. Schwarz, R.U., R.L., L.T.W., O.A.A., A.M.-L., M.O.B. and E. Sarisik critically revised the manuscript for important intellectual content. All authors read and approved the final manuscript.

Competing interests

N.K. owns issued patent no. US20160192889A1 ('Adaptive pattern recognition for psychosis risk modeling'). As a member of the Spring

Health's Scientific Advisory Board, N.K. has advised the company on the development of tools to predict treatment outcomes for depression and psychosis. He has no equity and has received no financial compensation from this company. A.B. reports speaker fees from Otsuka, Lundbeck, Angelini and ROVI outside the submitted work. J.H. reports personal fees from Orion, Lundbeck and Otsuka, and others from Takeda during the conduct of the study. R.U. reports speaker fees from Sunovion, Otsuka and Vitaris outside the submitted work and unpaid officership with the British Association for Pharmacology (Honorary General Secretary 2021–2024). She serves as Deputy Editor for the *British Journal of Psychiatry*. P.F. has received research support/honoraria for lectures or advisory activities from Boehringer-Ingelheim, Janssen, Lundbeck, Otsuka, Recordati and Richter outside the submitted work. O.A.A. is a consultant to Cortechs.ai and has received speaker's honoraria from Otsuka, Lundbeck, Janssen and Sunovion. R.L. reports honoraria for lectures or advisory activities from Boehringer-Ingelheim, Janssen, Otsuka and ROVI outside the submitted work. The other authors declare no competing interests.

Additional information

Supplementary information The online version contains supplementary material available at https://doi.org/10.1038/s44220-025-00522-3.

Correspondence and requests for materials should be addressed to Nikolaos Koutsouleris.

Peer review information *Nature Mental Health* thanks Udo Dannlowski, Yingkai Yang and the other, anonymous reviewer(s) for their contribution to the peer review of this work.

[1]Department of Psychiatry and Psychotherapy, Ludwig-Maximilian-University, Munich, Germany. [2]International Max Planck Research, School for Translational Psychiatry (IMPRS-TP), Munich, Germany. [3]Max-Planck Institute of Psychiatry, Munich, Germany. [4]Department of Psychology, University of Oslo, Oslo, Norway. [5]Section for Precision Psychiatry, Division of Mental Health and Addiction, Oslo University Hospital & Institute of Clinical Medicine, University of Oslo, Oslo, Norway. [6]K.G. Jebsen Center for Neurodevelopmental Disorders, University of Oslo, Oslo, Norway. [7]Department of Psychiatry and Psychotherapy, Central Institute of Mental Health, Medical Faculty, Mannheim, Heidelberg University, Mannheim, Germany. [8]DZPG (German Centre for Mental Health), Partner site Mannheim/Ulm/Heidelberg, Heidelberg, Germany. [9]Department of Psychiatry and Psychotherapy, University of Cologne, Cologne, Germany. [10]Department of Psychiatry, University of Turku, Turku, Finland. [11]Department of Basic Medical Science, Neuroscience and Sense Organs, University of Bari Aldo Moro, Bari, Italy. [12]Department of Psychiatry and Psychotherapy, University of Lübeck, Lübeck, Germany. [13]Department of Psychiatry (Psychiatric University Hospital, UPK), University of Basel, Basel, Switzerland. [14]Department of Neurosciences and Mental Health, Fondazione IRCCS Ca' Granda Ospedale Maggiore Policlinico, Milan, Italy. [15]Department of Pathophysiology and Transplantation, University of Milan, Milan, Italy. [16]Institute of Mental Health, University of Birmingham, Birmingham, UK. [17]Early Intervention Service, Birmingham Women's and Children's NHS Foundation Trust, Birmingham, UK. [18]Department of Psychiatry, University of Oxford, Oxford, UK. [19]NIHR Oxford Health Biomedical Research Centre, University of Oxford, Oxford, UK. [20]School of Psychology, University of Birmingham, Birmingham, UK. [21]Centre for Youth Mental Health, University of Melbourne, Melbourne, Victoria, Australia. [22]Orygen, Melbourne, Victoria, Australia. [23]Institute for Translational Psychiatry, University Muenster, Muenster, Germany. [24]Department of Psychiatry and Psychotherapy, Medical Faculty, Heinrich-Heine University, Düsseldorf, Germany. [25]DZPG (German Centre for Mental Health), Partner site Munich/Augsburg, Munich, Germany. [26]Hector Institute for Artificial Intelligence in Psychiatry, Central Institute of Mental Health, Medical Faculty, Mannheim, Heidelberg University, Mannheim, Germany. [27]Institute of Psychiatry, Psychology and Neuroscience, King's College London, London, UK. [28]These authors contributed equally: Adyasha Khuntia, David Popovic, Ariane Wiegand, Nikolaos Koutsouleris.
✉e-mail: nikolaos.koutsouleris@med.uni-muenchen.de

nature portfolio

Corresponding author(s): Nikolaos Koutsouleris

Last updated by author(s): Aug 21, 2025

Reporting Summary

Nature Portfolio wishes to improve the reproducibility of the work that we publish. This form provides structure for consistency and transparency in reporting. For further information on Nature Portfolio policies, see our Editorial Policies and the Editorial Policy Checklist.

Statistics

For all statistical analyses, confirm that the following items are present in the figure legend, table legend, main text, or Methods section.

n/a	Confirmed
☐	☒ The exact sample size (*n*) for each experimental group/condition, given as a discrete number and unit of measurement
☐	☒ A statement on whether measurements were taken from distinct samples or whether the same sample was measured repeatedly
☐	☒ The statistical test(s) used AND whether they are one- or two-sided *Only common tests should be described solely by name; describe more complex techniques in the Methods section.*
☐	☒ A description of all covariates tested
☐	☒ A description of any assumptions or corrections, such as tests of normality and adjustment for multiple comparisons
☐	☒ A full description of the statistical parameters including central tendency (e.g. means) or other basic estimates (e.g. regression coefficient) AND variation (e.g. standard deviation) or associated estimates of uncertainty (e.g. confidence intervals)
☐	☒ For null hypothesis testing, the test statistic (e.g. *F*, *t*, *r*) with confidence intervals, effect sizes, degrees of freedom and *P* value noted *Give P values as exact values whenever suitable.*
☒	☐ For Bayesian analysis, information on the choice of priors and Markov chain Monte Carlo settings
☐	☒ For hierarchical and complex designs, identification of the appropriate level for tests and full reporting of outcomes
☐	☒ Estimates of effect sizes (e.g. Cohen's *d*, Pearson's *r*), indicating how they were calculated

Our web collection on statistics for biologists contains articles on many of the points above.

Software and code

Policy information about availability of computer code

Data collection	No data have been explicitly collected for this specific study.; only pre-existing datasets were used. MRI image processing was conducted using VBM8, with detailed settings provided in the Supplementary Material. The exact SPM batch file with all parameters is available upon request from the corresponding author. All other analysis code is available via the GitHub repository.
Data analysis	NeuroMiner 1.2 (https://neurominer-git.github.io/NeuroMiner_1.2/intro.html), SPLS Toolbox (https://github.com/dpopovic30/spls_toolbox_compiled), MATLAB R2022a, MATLAB R2023b, R version 4.4.1, RStudio Version 2024.12.1+563, and VBM8 were used in the analyses. The NeuroMiner template files detailing the machine learning analysis setup are described in the manuscript and the exact template files may be available upon request from the corresponding author.

For manuscripts utilizing custom algorithms or software that are central to the research but not yet described in published literature, software must be made available to editors and reviewers. We strongly encourage code deposition in a community repository (e.g. GitHub). See the Nature Portfolio guidelines for submitting code & software for further information.

Data

Policy information about availability of data

All manuscripts must include a data availability statement. This statement should provide the following information, where applicable:

- Accession codes, unique identifiers, or web links for publicly available datasets
- A description of any restrictions on data availability
- For clinical datasets or third party data, please ensure that the statement adheres to our policy

Parts of the data, including the IXI dataset (https://brain-development.org/ixi-dataset/) and the Cambridge Centre for Ageing and Neuroscience (CAM-CAN) dataset (https://camcan-archive.mrc-cbu.cam.ac.uk), are accessible to researchers upon request from the respective repositories. Other datasets (PRONIA, MUC, NORMENT) analyzed during the current study are not publicly available due to data sharing restrictions defined in the participants' signed informed consent agreements. Trained models are available from the corresponding author upon reasonable request.
The code supporting the findings of this study is available via GitHub at https://github.com/adyasha95/BMIgapCodeRepo.

Research involving human participants, their data, or biological material

Policy information about studies with human participants or human data. See also policy information about sex, gender (identity/presentation), and sexual orientation and race, ethnicity and racism.

Reporting on sex and gender	The term sex is used in the manuscript to describe biological attributes. Both males and females were included in the study, with group-specific numbers reported. Sex-specific analyses were performed, with male and female groups separately assessed for the association between weight change and BMIgap.
Reporting on race, ethnicity, or other socially relevant groupings	Race and ethnicity data were not consistently collected across all cohorts and were therefore not included in the analysis.
Population characteristics	The study included 1504 healthy controls (HC; discovery: N=770, mean age=41.3±15.5 years, 56.5% female; validation: N=734, mean age=32.2±12.8 years, 50.8% female; Cam-CAN: N=536, mean age=54.3±18.6 years, 48.7% female), 146 individuals with schizophrenia (N=146, mean age=30.8±10.0 years, 23.3% female), 213 with clinical high-risk states (CHR; N=213, mean age=23.9±5.2 years, 48.4% female), and 200 with recent-onset depression (ROD; N=200, mean age=26.0±6.4 years, 48.0% female).
Recruitment	Participants included are from independent datasets covering 15 sites: Information eXtraction from Images (IXI; https://brain-development.org/ixi-dataset/), Personalized Prognostic Tools for Early Psychosis Management (PRONIA; www.pronia.eu), Norwegian Centre for Mental Disorders Research (https://www.med.uio.no/norment/), the Munich Brain Imaging Database and Cambridge Centre for Ageing and Neuroscience dataset. Patients with schizophrenia were assessed using the Structured Clinical Interview for DSM-IV Axis I Disorders (SCID). Recent-onset depression (ROD) was defined as a first major depressive episode within the past three months, determined by SCID. Clinical high-risk (CHR) states were defined by cognitive disturbances assessed with the Schizophrenia Proneness Instrument and/or ultra-high-risk criteria based on the Structured Interview for Psychosis-Risk Syndromes. For CHR and ROD groups, only minimal antipsychotic medication use was permitted.
Ethics oversight	Ethical approval was obtained from the institutional review boards or ethics committees at each participating site. All participants provided written informed consent in accordance with the Declaration of Helsinki.

Note that full information on the approval of the study protocol must also be provided in the manuscript.

Field-specific reporting

Please select the one below that is the best fit for your research. If you are not sure, read the appropriate sections before making your selection.

☒ Life sciences ☐ Behavioural & social sciences ☐ Ecological, evolutionary & environmental sciences

For a reference copy of the document with all sections, see nature.com/documents/nr-reporting-summary-flat.pdf

Life sciences study design

All studies must disclose on these points even when the disclosure is negative.

Sample size	Sample size was determined based on availability of suitable data across multiple independent cohorts. While no formal a priori power calculation was performed, the inclusion of 770 healthy controls for model training, 734 for validation, 536 for external validation, and 559 clinical participants (146 SCZ,213 CHR, 200 ROD) provided sufficient power for predictive modeling and subgroup comparisons. Reporting follows the TRIPOD guidelines.
Data exclusions	Participants were excluded if T1-weighted MRI data were missing, of insufficient quality (e.g., motion artifacts), or failed preprocessing steps such as segmentation or normalization in the VBM8 pipeline. Exclusion criteria were pre-specified and consistently applied across all sites.
Replication	The model was validated in two independent healthy control cohorts (HCvalidation and HCCam-CAN) to test generalizability and

Replication	reproducibility of the findings. Results were further applied to three clinical samples (SCZ, CHR, ROD), with consistent patterns observed across subgroups. All model evaluation steps were conducted within a strict nested cross-validation framework to ensure generalizability.
Randomization	Randomization was not applicable, as this was an observational, non-interventional study using previously collected clinical and neuroimaging data. No random group allocation or experimental manipulation was involved.
Blinding	Blinding was not applicable in this observational study. However, data preprocessing and model training were fully automated and performed using nested cross-validation to prevent information leakage between training and test data.

Reporting for specific materials, systems and methods

We require information from authors about some types of materials, experimental systems and methods used in many studies. Here, indicate whether each material, system or method listed is relevant to your study. If you are not sure if a list item applies to your research, read the appropriate section before selecting a response.

Materials & experimental systems

n/a	Involved in the study
☒	☐ Antibodies
☒	☐ Eukaryotic cell lines
☒	☐ Palaeontology and archaeology
☒	☐ Animals and other organisms
☐	☒ Clinical data
☒	☐ Dual use research of concern
☒	☐ Plants

Methods

n/a	Involved in the study
☒	☐ ChIP-seq
☒	☐ Flow cytometry
☐	☒ MRI-based neuroimaging

Clinical data

Policy information about clinical studies

All manuscripts should comply with the ICMJE guidelines for publication of clinical research and a completed CONSORT checklist must be included with all submissions.

Clinical trial registration	The study is not part of any clinical trials
Study protocol	This study combined data from multiple sources. Data from the PRONIA consortium (www.pronia.eu) were collected following a standardized, multicenter recruitment and assessment protocol across sites in Finland, Germany, Italy, Switzerland, and the United Kingdom. Data from the Cam-CAN project (www.cam-can.org) and the IXI dataset (https://brain-development.org/ixi-dataset/) are publicly available and were collected according to their respective study protocols, available on their websites. Data from the NORMENT Centre for Mental Disorders Research (www.med.uio.no/norment/english/) were collected under local ethics approvals at the University of Oslo and Oslo University Hospital, following standardized clinical and MRI acquisition protocols. Data from the Munich Brain Imaging Database were collected under institutional guidelines and ethical approvals at LMU Munich. Standardized MRI and clinical assessment protocols were followed across sites where applicable. All participants provided written informed consent in accordance with the Declaration of Helsinki.
Data collection	No data have been collected during this specific study. We have used only existing and existing datasets in this study. For PRONIA, participants underwent baseline and follow-up assessments every three months. Public datasets (Cam-CAN and IXI) provide cross-sectional demographic, cognitive, and MRI data collected at their respective sites. NORMENT and MUC datasets included clinical participants and healthy controls recruited through clinical services and community outreach, with corresponding MRI and clinical evaluations. Patients with schizophrenia were assessed using the Structured Clinical Interview for DSM-IV Axis I Disorders (SCID). Recent-onset depression (ROD) was defined as a first major depressive episode within the past three months, determined by SCID. Clinical high-risk (CHR) states were defined by cognitive disturbances assessed with the Schizophrenia Proneness Instrument and/or ultra-high-risk criteria based on the Structured Interview for Psychosis-Risk Syndromes. For CHR and ROD groups, only minimal antipsychotic medication use was permitted.
Outcomes	The primary outcome was the brain-based deviation from expected BMI (BMIgap), derived from structural MRI data to capture neurobiological markers of metabolic vulnerability. Secondary outcomes included clinical symptom scores, functional outcomes, and future weight change trajectories, depending on cohort data availability.

Plants

Seed stocks: NA

Novel plant genotypes: NA

Authentication: NA

Magnetic resonance imaging

Experimental design

Design type: Structural MRI, resting state (no task)

Design specifications: Structural T1-weighted images were acquired across multiple sites using standardized protocols. No experimental trials or tasks were administered; the MRI sessions consisted solely of anatomical scans.

Behavioral performance measures: NA

Acquisition

Imaging type(s): Structural (T1-weighted MRI)

Field strength: 1.5 Tesla and 3 Tesla scanners were used across different sites.

Sequence & imaging parameters: High-resolution T1-weighted anatomical scans were obtained using different MRI scanners (Siemens, Philips, GE). Voxel sizes ranged from 0.45×0.45×1.5 mm^3 to 1×1×1 mm^3. Field of View (FOV) ranged approximately between 230×230 mm^2 and 288×288 mm^2.
Typical TR: 2000–2730 ms;
TE: 2.28–5.5 ms;
Flip Angle: 7°–12°.
Pulse sequences varied slightly across scanners but were all optimized for structural brain imaging.
(details in the Supplement Methods)

Area of acquisition: Whole-brain anatomical scans covering the entire brain volume were acquired.

Diffusion MRI ☐ Used ☒ Not used

Preprocessing

Preprocessing software: VBM8 toolbox (http://dbm.neuro.uni-jena.de/vbm) implemented in SPM.
Steps included: bias correction, tissue classification, normalization to MNI-space, modulation by non-linear components only, and reslicing to 3×3×3 mm^3 isotropic voxel size for computational efficiency and noise reduction.

Normalization: Images were normalized to MNI space using a unified model with both linear (12-parameter affine) and non-linear transformations, including high-dimensional DARTEL normalization.

Normalization template: MNI standard space template (as implemented in VBM8).

Noise and artifact removal: Bias correction was applied to correct for intensity inhomogeneities.
An absolute masking threshold of 0.1 was used to exclude voxels of non-grey matter tissues. No explicit motion correction was necessary as only structural MRI data were analyzed.

Volume censoring: NA

Statistical modeling & inference

Model type and settings: Multivariate predictive modeling using machine learning (support vector regression) within a normative modeling framework. Five-fold repeated nested cross-validation with five permutations at inner and outer loops to prevent overfitting and information leakage.

Effect(s) tested

Individualized prediction of BMI from voxel-wise GMV patterns across healthy and clinical populations; deviation scores (BMIgap) were analyzed across diagnostic groups.

Specify type of analysis: ☒ Whole brain ☐ ROI-based ☐ Both

Statistic type for inference

Voxel-wise analysis.

(See Eklund et al. 2016)

Correction

False Discovery Rate (FDR) correction for multiple comparisons.

Models & analysis

n/a	Involved in the study
☒	☐ Functional and/or effective connectivity
☒	☐ Graph analysis
☐	☒ Multivariate modeling or predictive analysis

Multivariate modeling and predictive analysis

Vol-wise grey matter volume (GMV) was used as the independent variable (71276 features per subject).
Feature extraction and dimensionality reduction were performed using principal component analysis (PCA) at different energy thresholds (0.25, 0.50, 0.75) during cross-validation.
Model training was performed using v-support vector regression (v-SVR) with a linear kernel.
A repeated nested five-fold cross-validation with five permutations was used to prevent overfitting and ensure model generalizability. Model evaluation was based on the mean absolute error (MAE) as the performance metric. Statistical significance of the model performance was assessed using 1000 label permutations ($\alpha = 0.05$).
The final predictive brain patterns were visualized based on cross-validation ratio and sign-consistency mapping.